Caspase-mediated cleavage of Murine Norovirus NS1/2 potentiates apoptosis and is required for persistent infection

Bridget A. Robinson[1], Broc T McCune[2], A. Mack Peters[1], and Timothy J. Nice[1]*

[1]Department of Molecular Microbiology and Immunology, Oregon Health and Science University, Portland, Oregon, USA

[2]Department of Microbiology, University of Texas Southwestern Medical Center, Dallas, TX, USA

*Correspondence: Timothy J. Nice, nice@ohsu.edu

Short title: Cleavage of MNV NS1/2 potentiates apoptosis and is required for persistence

Abstract

Human norovirus (HuNoV) is the leading cause of acute gastroenteritis and is spread by fecal shedding that can often persist for weeks to months after infection. Murine norovirus (MNV) is also shed persistently in the feces and provides a tractable model to study molecular mechanisms of enteric persistence. Previous studies have identified non-structural protein 1 (NS1) from the persistent MNV strain CR6 as critical for persistent infection in intestinal epithelial cells (IECs), but its mechanism of action remains unclear. We now find that the function of NS1 in promoting persistence is regulated by apoptosis. Following induction of apoptosis in infected cells, a minority of NS1 is cleaved from the precursor NS1/2 protein, and this cleavage is prevented by mutation of caspase target motifs. MNV strain CR6 with these mutations ($CR6_{\Delta casp}$) is profoundly compromised in infection of IECs and persistence in the intestine. Conversely, replication in tissues outside of the intestine, or in a cultured macrophage cell line, is unchanged, indicating that the requirement of NS1/2 cleavage is intestine-specific. Intriguingly, we also find that cleavage of CR6 NS1/2 potentiates apoptosis, suggesting that regulation of cell death is a novel function of this viral protein. Together, these data indicate that the ability of NS1 to promote MNV persistence in IECs is regulated by host caspases, and suggest that potentiation of apoptosis plays a role in viral tropism in the intestine.

Author Summary

Human Norovirus infection is highly contagious and the most common cause of acute gastroenteritis. Norovirus can persist and be shed for months after infection, leading to continued outbreaks. There are many unanswered questions as to host and viral components of norovirus pathogenesis that can be addressed within the murine norovirus (MNV) model system. We previously identified a critical role for a viral protein, NS1, for intestinal persistence. Herein we describe how the regulation of NS1 is critical for persistent infection in intestinal epithelial cells, but is not required for acute infection of non-epithelial cells, or infection of tissues outside of the gut. Additionally, we demonstrate that NS1 is both regulated by the host cell death machinery, and also reciprocally regulates that machinery to promote cell death during MNV infection, and found that this is specific to persistent strain of MNV. Altogether these data identify a role for how NS1 in a new pathway involved in establishing a persistent norovirus infection in the intestine.

46 **Introduction**

47 Human norovirus (HuNoV) is the most common cause of epidemic gastroenteritis, and can be
48 particularly dangerous for infants and the elderly [1,2]. Persistent viral shedding often occurs for weeks to
49 months after acute infection, even in asymptomatic individuals [3,4], and is a potential source for continued
50 outbreaks. Despite recent advances in culture systems to study HuNoV [5,6], there is still not an efficient
51 *in vitro* or small animal system for investigating the molecular components of HuNoV infection.
52 Fortunately, HuNoV and murine norovirus (MNV) share genotypic (ssRNA, positive-sense, ~7.5kb
53 genome) and phenotypic (fecal-oral transmission, persistence in intestinal epithelial cells (IECs), and
54 shedding in the feces) similarities, and utilization of the MNV model system has considerably advanced
55 our molecular understanding of norovirus pathogenesis and persistence [7-9].

56 All noroviruses encode six non-structural proteins (NS1/2, NS3, NS4, NS5, NS6, and NS7)
57 expressed upon cleavage of the open reading frame 1 (ORF 1) polyprotein by the viral NS6 protease [10]
58 and two structural capsid proteins (VP1 and VP2) from ORFs 2 and 3 [11,12], respectively. MNV also has
59 a fourth ORF that encodes a unique virulence factor not present in HuNoV [13]. Although the non-structural
60 protein NS1/2 is not cleaved by the viral protease, it can be cleaved into two additional proteins (NS1 and
61 NS2) [10,14] by the host protease, caspase 3 [10]. However, definitive data regarding the extent and
62 consequences of such caspase cleavage are lacking.

63 Prior comparison of an acute and a persistent strain of MNV identified two viral proteins that are
64 key components of MNV pathogenesis and persistence [15-17]: the major capsid protein (VP1) of the acute
65 strain CW3 ($VP1^{CW3}$) drives viral dissemination outside of the intestine, and NS1 of the persistent strain
66 CR6 ($NS1^{CR6}$) is critical for viral persistence in the intestine. Additional *in vivo* analyses demonstrated
67 $NS1^{CR6}$ is absolutely required for infection of a specialized type of IEC, the tuft cell, identified as the cellular
68 reservoir for MNV persistence [18]. Despite the differences in systemic spread and intestinal persistence,
69 both CW3 and CR6 can infect macrophages, dendritic cells, T-cells, and B-cells *in vitro* and *in vivo*
70 [6,19,20], and utilize the same cell-surface receptor, CD300lf [21,22]. Thus, $VP1^{CW3}$ and $NS1^{CR6}$ are

71 functioning via mechanisms other than receptor usage and replicative capacity to promote viral
72 dissemination and persistence.

73 In addition to identified roles of viral proteins in norovirus pathogenesis, critical aspects of the host
74 anti-viral response have also been identified. Particularly important is the multi-faceted interferon (IFN)
75 response [23]. Type I (α/β) and type III (λ) IFNs are both key players in the innate anti-viral response,
76 primarily distinguished by the differential expression of their respective receptors [23]. The IFN-α/β
77 receptor is widely expressed on most cell types, whereas the IFN-λ receptor is predominantly expressed on
78 epithelial cells. In regards to MNV, IFN-α/β signaling is critical for control of MNV in myeloid cells,
79 demonstrated by increased titers in macrophages that do not express the IFN-α/β receptor [19], the inability
80 to control systemic MNV infection in mice that specifically lack IFN-α/β receptor expression on myeloid
81 cells [24,25], and increased dissemination and lethality in mice that do not express the downstream signaling
82 molecule, STAT1 [11]. In contrast to systemic spread, intestinal MNV infection is controlled by IFN-
83 λ signaling in IECs, and persistent infection can be cleared and prevented with IFN-λ treatment [26,27].
84 Interestingly, recent data suggests that $NS1^{CR6}$ may have a role in antagonizing the IFN-λ response during
85 intestinal infection of IECs [28], but how $NS1^{CR6}$ may function in this capacity and whether this is its sole
86 function during persistent infection is unknown.

87 In addition to the IFN response, host cells also initiate apoptosis as a means of eliminating virus-
88 infected cells. Correspondingly, viruses have evolved ways to hijack apoptotic machinery to their benefit.
89 Apoptosis is a non-inflammatory, highly-regulated disassembly of the cell mediated by a family of cysteine
90 proteases (caspases), and culminates in the release of the cellular contents within membranous vesicles
91 (apoptotic bodies) that are taken up by professional phagocytes, as well as neighboring cells [29]. Because
92 induction of apoptosis is an innate response to stress or infection, most viruses have developed ways to
93 delay apoptosis in an effort to maximize viral progeny [30], exemplified by a number of large DNA viruses
94 that encode viral homologs of the cellular anti-apoptotic protein, Bcl-2 [31]. Conversely, influenza virus
95 actively induces apoptosis through manipulation of other Bcl-2 family proteins, which increases viral

96 replication and enhances pathogenesis [32,33]. In addition to manipulating apoptosis to prevent cell death
97 or increase viral progeny, a number of viruses, including picornaviruses and flaviviruses, utilize 'apoptotic
98 mimicry' as an alternate mode of egress and viral dissemination [34], and some viruses rely on apoptotic
99 caspases to cleave viral proteins as an additional level of regulation [35-37]. Thus, apoptosis can be both
100 anti-viral and pro-viral, making its regulation critical for viral pathogenesis.

101 HuNoV and MNV infection both induce apoptosis, as indicated by association with markers of
102 apoptosis in infected intestinal tissue [38-40]. Thus, these viruses have likely also developed mechanisms
103 to regulate apoptosis to promote infection. Apoptosis in MNV-infected myeloid cells includes
104 downregulation of an inhibitor of apoptosis protein, survivin, and activation of caspases and other cysteine
105 proteases [41,42]. Furthermore, independent expression of the MNV ORF1 polyprotein, which encodes
106 the non-structural proteins (including NS1/2), is also sufficient to induce apoptosis [43], indicating one or
107 more non-structural proteins could be promoting apoptosis during infection. Additional analyses of the
108 non-structural proteins identified two functional caspase motifs in NS1/2, and demonstrated that the NS1/2
109 protein can be cleaved by recombinant caspase 3 in a cell-free system [10]. Based on these published data,
110 apoptosis during MNV infection may be facilitated by one or more non-structural proteins, and the virus
111 may benefit from apoptotic signaling via utilization of a host caspase to regulate expression of NS1, the
112 critical determinant for intestinal persistence [15].

113 Herein, we further delineate how $NS1^{CR6}$ functions to promote viral persistence by characterizing
114 NS1/2 cleavage during MNV infection and its role in intestinal persistence. We demonstrate that at late
115 times post-infection, concurrent with induction of apoptosis, a minority of total NS1/2 protein is cleaved in
116 a caspase-dependent manner. Despite the relatively low proportion of total NS1/2 that is cleaved, our data
117 demonstrate that $NS1/2^{CR6}$ cleavage is absolutely required for persistent infection in IECs, and this involves
118 a function separate from IFN antagonism. Moreover, the cleavage of $NS1/2^{CR6}$ potentiates apoptotic cell
119 death *in vitro,* suggesting controlled induction of apoptosis is a novel mechanism required for infection of
120 IECs and intestinal persistence.

121

122

123 **Results**

124 **Host caspases cleave NS1/2 at late times post-infection**. Previous cell-free studies identified two
125 functional caspase motifs (DKAD^{121} and DAMD^{131}) within NS1/2 that are cleaved by host caspase 3 [10]
126 (Fig 1A), however, the necessity and utility of these sites during viral infection was unknown. Therefore,
127 to assess the role of NS1/2 cleavage during viral persistence, we mutated these sites ($D_{121}G$ and $D_{131}G$)
128 within the persistent MNV strain, CR6, and named this virus $CR6_{\Delta casp}$ (Fig 1B). Analyses of viral protein
129 expression during MNV infection of BV2 cells demonstrates cleavage of a minority of total NS1/2 protein
130 at late times post-infection with both an acute (CW3) and persistent (CR6) strain of MNV (Fig 1C).
131 Cleavage of NS1/2 did not occur in $CR6_{\Delta casp}$-infected cells, demonstrating that it is dependent on the caspase
132 motifs (Fig 1C), and, importantly, these mutations did not disrupt overall expression of full-length NS1/2
133 protein. To determine whether host caspases are responsible for NS1/2 cleavage, cells were treated at 10h
134 post-infection (PI) with a pan-caspase inhibitor, ZVAD-fmk, and indeed, the ~28kDa NS2 protein was no
135 longer detected in infected cells at late times post-infection (Fig 1D). The ~18kDa NS1 protein was
136 inconsistently detected in cells via western blot and may be a technical result of the small amounts of overall
137 NS1/2 that get cleaved during infection. Together, these data demonstrate that a small portion of total NS1/2
138 protein is cleaved by host caspases at relatively late times post-infection with MNV.

139

140 **Cleavage of NS1/2 is not required for viral replication *in vitro*.** The abundance of full-length NS1/2
141 following infection with $CR6_{\Delta casp}$ indicated that viral protein production was not dependent on these
142 cleavage motifs (Fig 1C, D). To further assess whether NS1/2 cleavage is necessary for production of
143 infectious virus, we compared plaque forming units (PFU) produced from cell cultures infected with CR6
144 vs. $CR6_{\Delta casp}$ over a 48h time course. Inhibition of NS1/2 cleavage did not significantly impair CR6
145 replication in BV2 cells (Fig 2A), or within wildtype (WT) bone-marrow derived macrophages (BMDCs)
146 (Fig 2C).

147 Our *in vivo* analyses discussed in the following section aimed to assess the role of NS1/2 cleavage
148 on systemic replication as well as intestinal replication of MNV; therefore, we generated CR6 and CR6$_{\Delta casp}$
149 viral strains that could spread systemically due to chimeric expression of VP1^{CW3} (Fig 1B) [15]. We
150 performed growth curves using these capsid chimeras in parallel with growth curves for CR6 and CR6$_{\Delta casp}$
151 described above. *In vitro* growth kinetics in BV2 cells and WT BMDCs displayed minimal differences
152 between CR6-VP1^{CW3} and CR6$_{\Delta casp}$-VP1^{CW3} (Fig 2B, D). The minor, yet significant, decrease in peak titers
153 of CR6$_{\Delta casp}$-VP1^{CW3} compared to CR6-VP1^{CW3} in WT BMDCs but not in BV2 cells indicated NS1/2
154 cleavage may serve a critical function specific to BMDC cultures. Recently published data suggests a role
155 for NS1^{CR6} in IFN antagonism, therefore, we assessed whether NS1/2 cleavage affected growth in BMDC
156 cultures that are not responsive to IFN (*Stat1*$^{-/-}$ BMDCs). All the MNV strains we analyzed demonstrated
157 higher peak titers in *Stat1*$^{-/-}$ BMDCs compared to WT BMDCs (Fig 2C-F), confirming the known inhibitory
158 effect of IFNs on MNV replication [19], and the decreased replicative capacity of CR6$_{\Delta casp}$-VP1^{CW3} was no
159 longer evident (compare Fig 2D to 2F). Altogether, these data indicate that NS1/2 cleavage is not necessary
160 for viral replication but may play a role in counteracting the IFN response.
161
162 **NS1/2 cleavage is critical for persistence in the intestine**. To analyze whether NS1/2 cleavage impacts
163 MNV infection of systemic and intestinal tissues *in vivo*, we perorally challenged WT B6 mice with 1e6
164 PFU CR6, CR6$_{\Delta casp}$, CR6-VP1^{CW3} or CR6$_{\Delta casp}$-VP1^{CW3}, and analyzed tissues at three days post-infection
165 (dpi) for the presence of infectious virus (Fig 3A-D). As expected, CR6 and CR6-VP1^{CW3} were detected
166 within the mesenteric lymph node (MLN), ileum (devoid of Peyer's patches), and colon, the eventual site
167 of persistence (Fig 3A, B). Consistent with the high titers in intestinal tissue, we also detected infectious
168 virus shed in the feces of mice infected with CR6 and CR6-VP1^{CW3} at 3dpi (Fig 3C, D). However, in mice
169 infected with CR6$_{\Delta casp}$ or CR6$_{\Delta casp}$-VP1^{CW3}, we rarely detected infectious virus in intestinal tissues (Fig 3A,
170 B), nor being shed in the feces (Fig 3C, D), indicating that caspase cleavage of NS1/2 is required for
171 promoting early infection of the intestine.

172 Although production of infectious virus was severely compromised in intestinal tissues of MNV-
173 infected mice in the absence of NS1/2 cleavage, titers in the spleen were only modestly reduced and not
174 significantly different at 3dpi in the absence of NS1/2 cleavage (Fig 3B), indicating that NS1/2 cleavage is
175 not required for systemic spread. Similarly, we were able to detect MNV RNA within the Peyer's patches
176 of animals infected with CR6$_{\Delta casp}$-VP1^{CW3} using the ultra-sensitive *in situ* RNA hybridization platform,
177 RNAscope (Fig 3F), and this was not visibly different from CR6-VP1^{CW3}-infected mice (Fig 3E-G).
178 Together, these data suggest no requirement for NS1/2 cleavage during the initial infection in Peyer's
179 patches or for subsequent systemic spread (Fig 3B, spleen).

180 To further verify that NS1/2 cleavage is not required for systemic MNV infection and pathogenesis,
181 we infected *Stat1*$^{-/-}$ mice with either CR6-VP1^{CW3} or CR6$_{\Delta casp}$-VP1^{CW3} (Fig 3H). Previous work
182 demonstrated that VP1^{CW3} is critical for systemic spread [15,17], and lethality in *Stat1*$^{-/-}$ mice [16,17,24].
183 Accordingly, we found that peroral challenge with CR6-VP1^{CW3} resulted in lethal MNV infection in *Stat1*$^{-}$
184 $^{/-}$ mice, and although NS1/2 cleavage is critical for efficient infection in the intestine, CR6$_{\Delta casp}$-VP1^{CW3}
185 infection also resulted in 100% mortality in *Stat1*$^{-/-}$ mice (Fig 3H). As a control, we infected *Stat1*$^{-/-}$ mice
186 with CR6, which persists, but does not result in lethal infection (Fig 3H) [15]. Overall, our characterization
187 of acute infection demonstrates that NS1/2 cleavage is not required for systemic spread of MNV and is not
188 necessary for lethal pathology in *Stat1*$^{-/-}$ mice. However, NS1/2 cleavage is specifically required for
189 efficient MNV replication in the ileum (outside of Peyer's patches) and colon, the source of virus shed in
190 the stool and the site of eventual persistence.

191 Due to limited detection of virus at 3dpi in the intestinal tissues of mice infected with CR6$_{\Delta casp}$ and
192 CR6$_{\Delta casp}$-VP1^{CW3}, we predicted that these mutants would also fail to persist. Indeed, whereas CR6 or CR6-
193 VP1^{CW3} persisted in the ileum and colon at 21dpi (Fig 4A, B), and were shed in the stool (Fig 4C, D), we
194 rarely detected persistent virus in any tissues from mice infected with CR6$_{\Delta casp}$ or CR6$_{\Delta casp}$-VP1^{CW3} (Fig 4).
195 Altogether, these findings support a role for NS1/2 cleavage specifically within the intestinal tissue, and

196 temporally link the activity of NS1/2 cleavage to the first 3 days post-infection. Thus, NS1/2 cleavage is
197 required for establishing an infection in the intestine and subsequent persistence.
198
199 **NS1/2 cleavage functions independently of IFN.** Due to the dominant role IFN-λ plays in protection
200 against persistent MNV infection of the intestine [26], and the potential role of NS1/2 cleavage in
201 counteracting IFN signaling in BMDCs (Fig 2C, D compared to Fig 2E, F) [28], we sought to more
202 thoroughly characterize $CR6_{\Delta casp}$ infection in the absence of IFN-λ signaling. To this end, we infected WT
203 or *Ifnlr1*$^{-/-}$ mice with CR6 or $CR6_{\Delta casp}$ and monitored shedding in the stool over time (Fig 5A, B), and
204 persistence in the colon at 21dpi (Fig 5C, D). Additionally, to determine whether an early barrier to MNV
205 infection could be overcome with increased infectious dose, we included an experimental group with 10-
206 fold more $CR6_{\Delta casp}$ (1e7 PFU) in the inoculum. MNV was shed in all WT mice infected with CR6 beginning
207 on day 3 and continuing until the experimental endpoint, day 21. Consistent with the protective role of IFN-
208 λ, *Ifnlr1*$^{-/-}$ mice infected with CR6 shed greater than 10-fold more virus relative to WT mice (Fig 5A, B),
209 and CR6 was detected in colon tissue at levels commensurate with fecal shedding at 21dpi (Fig 5C, D). In
210 contrast, we were unable to detect shedding of $CR6_{\Delta casp}$ at any time from WT or *Ifnlr1*$^{-/-}$ mice (Fig 5A, B).
211 These data indicate that $NS1/2^{CR6}$ cleavage promotes persistent infection via a novel mechanism separate
212 from IFN antagonism.
213
214 **Cleavage of NS1/2 is critical for MNV infection of intestinal epithelial cells.** Our preceding data
215 demonstrated that disrupting NS1/2 cleavage leads to an overall reduction of infectious virus produced in
216 intestinal tissues of either WT (Figs 3, 4) or *Ifnlr1*$^{-/-}$ (Fig 5) mice. Therefore, to attain a more thorough
217 understanding of the role of NS1/2 cleavage on cellular tropism, we infected WT or knockout mice with
218 CR6 or $CR6_{\Delta casp}$ and analyzed infection of IECs at 3dpi by flow cytometry and RNAscope (Fig 6). We
219 concurrently quantified MNV infection of Peyer's patches by qPCR to enable contextualization of the IEC
220 infection data. We were able to detect viral RNA in Peyer's patches in the majority of CR6-infected mice

221 and ~50% of CR6$_{\Delta casp}$-infected mice (Fig 6A). Although CR6$_{\Delta casp}$ infection of Peyer's patches was less
222 robust than that of CR6, these data confirm that NS1/2 cleavage is not strictly required for initial infection
223 of non-epithelial cells during acute infection (Figs 3E-F, 6A). This detectable but reduced infection by
224 CR6$_{\Delta casp}$ was observed in mice deficient in IFN-λ receptor (*Ifnlr1*$^{-/-}$; LRKO), doubly-deficient in IFN-λ and
225 IFN-α/β receptors (*Ifnlr1*$^{-/-}$/*Ifnar1*$^{-/-}$; DKO), as well as receptor-sufficient controls (WT) (Fig 6A),
226 suggesting NS1/2 cleavage amplifies infection in Peyer's Patches.

227 To assess the requirement of NS1/2 cleavage in IEC infection, intestinal tissue devoid of Peyer's
228 patches was mechanically and enzymatically stripped to obtain a single cell suspension and stained for
229 CD45 and EpCAM as markers of immune cells and epithelial cells, respectively. The presence of MNV
230 infection was detected via dual intracellular staining using two distinct antibodies to NS1/2 in mice infected
231 with CR6 or CR6$_{\Delta casp}$ (Fig 6B, C). We analyzed IEC infection in the same mice as in Fig 6A, including
232 knockouts and littermate controls. Regardless of genotype, we only detected IEC infection when mice were
233 infected with CR6, but not CR6$_{\Delta casp}$ (Fig 6B, C). Additionally, tissue sections were examined via
234 RNAscope, and we reproducibly detected CR6 infection of IECs (Fig 6D, E), as well as non-epithelial cells
235 in the lamina propria (Fig 6E) but were unable to find evidence for CR6$_{\Delta casp}$ infection of IECs at 3dpi (Fig
236 6F). These data demonstrate the necessity of NS1/2 cleavage for CR6 infection of IECs, the cellular
237 reservoir of MNV persistence. Furthermore, the profound absence of CR6$_{\Delta casp}$ in IECs would translate to
238 a loss of IEC-dependent viral amplification and may explain the reduced titers in Peyer's patches (Fig 6A)
239 and MLN (Fig 3A, B) during acute infection. Altogether, our data demonstrate that eliminating IFN
240 signaling is not sufficient to rescue CR6$_{\Delta casp}$ infection of IECs (Figs 5 and 6), indicating that cleavage of
241 NS1/2 functions to promote persistent infection of IECs by a mechanism independent of the IFN-λ
242 response.
243

244 **NS1/2 cleavage promotes MNV-induced apoptosis.** We next sought to identify an IFN-λ-independent
245 cellular response altered by NS1/2 cleavage. Because apoptotic-associated caspases have been implicated
246 in cleavage of NS1/2 (Fig 1) [10], and NS1/2 cleavage is critical for developing a persistent MNV infection
247 (Figs. 4, 5), we postulated that apoptosis may be altered by NS1/2 cleavage to promote persistent infection
248 in the gut. Consistent with this hypothesis, we found that CR6 induced significantly more apoptosis in BV2
249 cells compared to $CR6_{\Delta casp}$ (Fig 7). This included an increase in the active form of caspase 3 (Fig 7A, B)
250 and an increase in PARP cleavage (Fig 7A), a known target of activated caspase 3 [44]. The increase in
251 caspase 3 activity at 18hpi (Fig 7B) was not simply due to increased infection in CR6-infected cultures, as
252 there were similar levels of ProPol detected in all infection conditions (Fig 7C). We also measured a
253 significant increase in cells expressing phosphatidylserine on the external plasma membrane via Annexin
254 V staining in CR6-infected cells (Fig 7E-G). Similarly, there was also an increase in these apoptotic
255 markers following infection with CR6 -$VP1^{CW3}$ compared to $CR6_{\Delta casp}$-$VP1^{CW3}$ (Fig 7D, E-H). Furthermore,
256 in support of the hypothesis that $NS1/2^{CR6}$ cleavage promotes apoptosis in a manner that is specific for
257 persistence, the acute strain of MNV, CW3, induced less apoptosis in all our analyses (Fig 7), despite
258 demonstrating NS1/2 cleavage (Fig 1C). Interestingly, CR6-$VP1^{CW3}$ infection resulted in increased cell
259 permeability and death relative to CR6 at 17hpi (Fig 7E, H), consistent with our separate findings that
260 $VP1^{CW3}$ drives lytic cell death and inflammatory cytokine production (Jacob VanWinkle, et al, manuscript
261 under review). However, even in the context of increased cell lysis associated with $VP1^{CW3}$, we still
262 observed a significant decrease in Annexin V-positivity in the absence of $NS1/2^{CR6}$ cleavage (Fig 7F, H),
263 suggesting NS1/2 cleavage is still promoting apoptosis even in the context of lysis and inflammation driven
264 by $VP1^{CW3}$. Together with the preceding data, these findings suggest that potentiation of apoptotic cell
265 death by caspase-mediated cleavage of NS1/2 is critical for determining IEC tropism and persistence.
266
267

268 **Discussion**

269 Herein, we demonstrate that caspase-mediated cleavage of the nonstructural protein, NS1/2, is
270 critical for developing a persistent MNV infection. We engineered and characterized a strain of MNV in
271 which NS1/2 is not cleaved ($CR6_{\Delta casp}$), and our *in vitro* and *in vivo* analyses demonstrate that NS1/2
272 cleavage is not required for viral replication in myeloid cells but is necessary for infection of IECs, the
273 eventual site of persistence. Furthermore, our data indicate that NS1/2 cleavage potentiates apoptosis,
274 suggesting apoptosis is a critical aspect of establishing a persistent MNV infection.

275 NS1/2 was not previously known to play a role in cell death during MNV infection, but is required
276 for viral replication beginning at the earliest stages of replication complex assembly. Norovirus replication
277 occurs in the cytoplasm on cellular membranes with a variety of organelle markers [45], and occurs near
278 membranous vesicles [19,45]. MNV NS1/2 targets to the endoplasmic reticulum (ER) [46,47] and promotes
279 replication via membrane re-organization and through an interaction with the vesicle-associated membrane
280 protein, VAPA [48,49]. Similarly, HuNoV NS1/2 also interacts with VAPA, targets to vesicles, and
281 disrupts vesicle trafficking when ectopically expressed [49]. Our data indicate that the functions of NS1/2
282 during viral replication remain intact when the caspase cleavage sites are mutated, and viral replication
283 occurs normally (Fig 2). NS1/2 cleavage only occurs after the bulk of viral replication has completed
284 indicating that its role in promoting apoptosis, IEC infection, and persistence involves relatively late events
285 in the viral lifecycle.

286 The last step of the viral replication cycle is egress. Therefore, NS1/2 cleavage and associated
287 apoptotic death may be important for regulating release of viral progeny. How noroviruses are released
288 from infected cells is not well understood, but infection of macrophages and DCs does result in cell lysis
289 [19], and non-enveloped viruses generally rely on cell lysis to release newly assembled virions. Death by
290 apoptosis may alter this process by reducing lytic virion release and favoring retention of virions within
291 cellular membranes. Indeed, a number of non-enveloped viruses utilize vesicle-associated egress as a
292 means of evasion from immune detection, and vesicles with exposed phosphatidylserine allow for

293 phagocytic uptake of novel target cells that may not express the viral receptor [50,51]. This type of vesicle
294 egress, known as 'apoptotic mimicry', is also utilized by enveloped viruses which can incorporate
295 phosphatidylserine directly into their viral envelope [34]. Viruses, or virus-filled vesicles, decorated with
296 phosphatidylserine can inhibit IFN responses via activation of Tyro3/Axl/Mer (TAM) receptor tyrosine
297 kinases when phagocytosed by dendritic cells (DCs) [52], which would allow more efficient viral
298 replication in those target cells. Thus, vesicular egress has the potential to dramatically change the outcome
299 of infection.

300 Previous work identified CD300lf as the MNV receptor [21], and accordingly, it is expressed on
301 MNV target cells, including myeloid cells and a specialized IEC subtype, tuft cells. Tuft cells are a rare
302 cell type in the intestinal epithelium and are dispersed among non-tuft IECs [53]. Interestingly, our analyses
303 often found intestinal villi with multiple, adjacent epithelial cells infected (Fig 6E) even though MNV
304 infection has not been shown to alter numbers of tuft cells in the intestine [18]. These findings raise the
305 possibility of receptor-independent transfer of MNV to neighboring IECs, which could be mediated by
306 apoptosis or vesicular egress regulated by NS1/2 cleavage. Future work will be necessary to determine
307 whether vesicle-associated egress occurs during norovirus infection and whether it is required for viral
308 persistence.

309 Regular maintenance of the highly proliferative intestinal epithelium means differentiated epithelial
310 cells have a short lifespan, and undergo a specialized form of apoptotic cell death (anoikis) triggered as the
311 cell detaches from the basal membrane and is shed into the lumen [54]. Specific Bcl-2 family proteins are
312 critical players in anoikis [55,56], and display increased expression as IECs transit up the villus [56]. It is
313 possible cleavage of NS1/2 (and perhaps NS1 directly) interferes with Bcl-2 family proteins as a means of
314 altering the kinetics of the highly-regulated pathways that control apoptosis within differentiated IECs.
315 Interestingly, similar to NS1/2 cleavage promoting apoptosis during infection, some Bcl-2 proteins (e.g.
316 Bid) are also regulated via cleavage, in which the truncated version is the active, pro-apoptotic form of the

317 protein [57]. It will be interesting to examine whether NS1/2 interactions with the apoptotic machinery
318 plays a role in maintaining IEC infection.

319 Death by apoptosis could also function to avoid immune detection and to limit inflammation
320 associated with cell lysis. Virus production that results from cell lysis would promote inflammatory signals
321 to alert the host of an infection. Thus, promotion of an apoptotic cell death in myeloid cells, mediated by
322 $NS1/2^{CR6}$ cleavage (Fig 7), would limit inflammation and benefit persistence. In addition to professional
323 phagocytes, phagocytosis by non-professional phagocytes (e.g. epithelial cells) is critical for efficient
324 clearance of apoptotic cells, and for limiting inflammation in tissues with high cellular turnover [58].
325 Specifically, in a mouse model of colonic injury, phagocytic uptake of apoptotic cells by IECs was sufficient
326 for limiting inflammation in the colon [59], and phagocytosis mediated by epithelial cells is similarly critical
327 for reducing inflammation in lung tissue [60] and mammary glands [61]. Thus, intestinal infection that
328 promotes apoptotic death and the phagocytic uptake by IECs would limit host detection and provide a non-
329 inflammatory environment that would allow more efficient infection of IECs and benefit MNV persistence.
330 Regardless of whether apoptotic death limits inflammation or functions by another mechanism, our studies
331 here have suggested potentiation of apoptosis following cleavage of NS1/2 as a new pathway critical for
332 sustained infection of IECs and expanded our understanding of the requirements for viral persistence in the
333 intestine.

334

335

336 **Materials and Methods**

337 **Cells, virus, and plaque assays**

338 BV2 cells (gift from Herbert Virgin IV, Washington University, St. Louis, MO), a mouse microglial
339 cell line [62], were maintained in DMEM (Life Technologies, ThermoFisher, Carslbad, CA) with 5% fetal
340 bovine serum (FBS) (VWR Seradigm, Radnor, PA), 1X Penicillin/Streptomycin/Glutamine (P/S/G)
341 solution, and 10mM HEPES. For bone-marrow derived dendritic cells (BMDCs), bone marrow was
342 isolated from the long bones of each hind leg of either a WT or *Stat1*$^{-/-}$ mouse and suspended in RPMI (Life
343 Technologies). Red blood cells were lysed using red blood cell lysis solution (Sigma, St Louis, MO) and
344 remaining bone marrow cells were cultured in RPMI with 10% FBS, 1X P/S/G solution, 10mM HEPES,
345 1X Sodium Pyruvate, 1X non-essential amino acids, and 20ng/mL GM-CSF obtained from supernatants of
346 GM-CSF-secreting cells (J558L, [63]). After seven days of culture (37C, 5% CO_2), non-adherent cells were
347 collected, infected with indicated MNV strains (MOI = 1), and maintained without GM-CSF. For indicated
348 experiments, ZVAD-fmk (Cell Signaling Technology [CST], Danvers, MA) was re-suspended in DMSO
349 and added to cells at 70µM. As a positive control for apoptosis assays, cells were treated with 1uM
350 staurosporine (SS) (CST) for 3.5h, at 37C.

351 CR6$_{\Delta casp}$ MNV was generated using site directed mutagenesis as previously described [15] with the
352 following primers: CR6 $D_{121}G$, 5'- GCCTAAGGAAGATAAAGCCG**G**TGCGCCCTCCCATGCG and
353 CR6 $D_{131}G$, 5'-TGCGGAGGACGCCATGG**G**TGCAAGGGAGCCCATAATTGG. The targeted residue
354 is underlined with the mutation in bold. Correct mutations were verified via sanger sequence analysis.

355 MNV stocks were generated from plasmids, as described [17]. Briefly, plasmids encoding viral
356 genomes of parental CW3 (GenBank accession no. EF014462.1), parental CR6 (GenBank accession
357 no. JQ237823), CR6-VP1^{CW3} [15,17] and the two NS1/2$_{\Delta casp}$ viral genomes generated herein, were
358 individually transfected into 293T cells (ATCC #CRL-3216). Forty-eight hours post-transfection, cells
359 were frozen, thawed, vortexed, and spun at 3,000xg to remove large debris. Supernatants were expanded

360 by two passages at MOI <0.05 in BV2 cells, and p2 virus supernatant was filtered (0.45um), concentrated
361 by ultra-centrifugation through a 30% sucrose cushion, and titered via plaque assay.
362 Plaque assays were performed in BV2 cells, similar to previously described methods [15]. Briefly,
363 BV2 cells were grown in 6well plates, infected with serial dilutions of each sample (500ul per well, 1h, RT,
364 on a rocking platform), after which the inoculum was removed and cells were overlaid with 1%
365 methylcellulose in complete DMEM. At 2-3d post-overlay, cells were fixed and stained with 20% EtOH /
366 0.1% crystal violet.
367
368 **Mice, infections, and tissue collection**
369 *Stat1*$^{-/-}$ (*Stat1*^{tm1Dlv}) mice were originally obtained from the Jackson Laboratories (stock #012606).
370 *Ifnlr1*$^{-/-}$ (generated from *Ifnlr1*$^{tm1a(EUCOMM)Wtsi}$) and *Ifnar1*$^{-/-}$ (*Ifnar1*^{tm1Agt}) were originally obtained from
371 Washington University in St. Louis. *Ifnlr1*$^{-/-}$ and *Ifnar1*$^{-/-}$ were bred to generate *Ifnlr1*$^{-/-}$/*Ifnar1*$^{-/-}$ mice (DKO)
372 and *Ifnlr1*$^{+/-}$/*Ifnar1*$^{+/-}$ (Dhet). Dhet and DKO crossbreeding yielded littermate mice deficient in neither
373 (Dhet), both (DKO), or a single (*Ifnlr1*$^{+/-}$/*Ifnar1*$^{-/-}$ or *Ifnlr1*$^{-/-}$/*Ifnar1*$^{+/-}$) IFN receptor gene(s); these
374 littermates were used for experiments to control for variability between litters.
375 All mice (7-9weeks old) were perorally infected with 1e6 PFU in a 25µL volume administered by
376 pipet, with the exception of experiments in Figure 6 where 1e6 or 1e7 PFU (as indicated in figure) was
377 administered by oral gavage in a 100µL volume. An equal proportion of males and females were
378 maintained among experimental groups to mitigate results due to any unidentified sex-dependent variables.
379 Same-sex mice, infected with the same MNV strain, were often co-housed for acute infection analyses (less
380 than three days), but singly-housed for extended experiments to prevent continued transmission between
381 animals.
382 Tissue samples, or a single fecal pellet, were collected in 2ml cryovials with 1mm zirconia/silica
383 beads (Biospec, Bartlesville, OK), frozen in a dry ice/EtOH bath and stored at -80C. For plaque assay or

384 RT-qPCR analyses, either 1ml DMEM or 1ml RiboZol (VWR) was added, respectively, and tissues were
385 homogenized via bead-beating (1min, RT) prior to continued analysis.
386
387 **Ethics Statement**
388 All mice were bred on C57BL/6 background and maintained in specific-pathogen-free barrier
389 facilities at Oregon Health & Science University under animal protocols approved by the institutional
390 animal care and use committee at Oregon Health & Science University (protocol # IP00000228) according
391 to standards set forth in the *Animal Welfare Act*.
392
393 **RNA, cDNA, and RT-qPCR**
394 RNA from tissues was extracted via RiboZol (VWR) protocols, and RNA from cells was extracted
395 with the ZR Viral RNA kit (Zymoresearch, Irvine, CA). DNA contamination was removed with Turbo
396 DNase (ThermoFisher), and 1ug of RNA was used to generate cDNA with the ImpromII reverse
397 transcriptase (Promega, Madison, WI). Quantitative PCR was performed using PerfeCTa qPCR FastMix
398 II (QuantaBio, Beverly, MA), and the following oligo/probes were used for detection: MNV genomic
399 RNA - Forward primer CACGCCACCGATCTGTTCTG, Reverse primer GCGCTGCGCCATCACTC,
400 and Probe TGCGCTTTGGAACAATGG; RPS29 - Forward primer GCAAATACGGGCTGAACATG,
401 Reverse primer GTCCAACTTAATG AAGCCTATGTC, and Probe CCTTCGCGTACTGCCGGAAGC.
402
403 **Cell Lysates and Western blot**
404 BV2 cells were grown and infected in 12well plates (2 e5 cells/well). Cells were lifted with
405 trypsin/0.25% EDTA (Gibco, ThermoFisher), washed with 1X cold PBS, resuspended in 100ul NP40 lysis
406 buffer (Alfo Aesar, Havervill, MA) with protease inhibitor cocktail (Sigma, St Louis, MO), incubated on
407 ice (15min with intermittent mixing), cleared via centrifugation (1min, 4C, full-speed), and diluted 1:1 with
408 2x SDS loading buffer (0.125 M Tris [pH 6.8], 4% SDS, 20% glycerol, 0.004% bromophenol blue, 10% β-

409 mercaptoethanol). Lysates were run on Novex Tris-Glycine gels (ThermoFisher), transferred to 0.2μm
410 PVDF (BioRad, Hercules, CA), blocked with 5% nonfat dry milk, and probed with the following antibodies
411 (Ab): caspase 3 pAb (CST), PARP pAb (CST), β-Actin pAb (Invitrogen), MNV NS1/2 pAb (a gift from
412 Dr. Vernon Ward, U. of Otago, Australia), or MNV ProPol pAb (a gift form Dr. Kim Green, NIH). Signal
413 was detected using goat, α-rabbit IgG-HRP (Jackson ImmunoResearch), developed with ECL substrate
414 (Pierce, ThermoFisher), and imaged with an ImageQuant LAS4000 (GE Healthcare, Little Chalfont, UK).
415

416 **Intestinal epithelial cell collection**

417 Epithelial fractions were prepared by non-enzymatic striping as previously described [24]. Mice
418 were euthanized and distal small intestine, cecum, and colon (regions of highest MNV replication) were
419 isolated. Peyer's patches were removed from small intestine and intestinal tissues were incubated in
420 stripping buffer (10% bovine calf serum, 15 mM HEPES, 5 mM EDTA, 5 mM dithiothreitol [DTT] in PBS)
421 with shaking for 20 min at 37°C. The dissociated cells were collected as the epithelial fraction, consisting
422 predominantly of IECs and directly used for flow cytometry.

423

424 **Surface and intracellular staining and flow cytometry**

425 BV2 cells were trypsinized and washed once with 1X PBS, stained with the amine-reactive viability
426 dye, Zombie Aqua (Biolegend, San Diego, CA) (20min, on ice), washed once with cold 2% FBS/PBS,
427 washed once with cold Annexin V binding buffer (CST), and stained with Annexin V-FITC (CST) (15min,
428 RT). Cells were immediately analyzed via flow cytometry on an LSR Fortessa (Becton Dickinson [BD],
429 Franklin Lakes, NJ) with FACSDiva software (BD), and data was analyzed using FlowJo software (FlowJo
430 LLC, Ashland, OR).

431 IECs isolated as described above were stained with the Zombie Aqua viability dye (Biolegend), Fc
432 receptors were blocked with purified CD16/CD32 pAb (clone93; Biolegend), and cells were probed for

433 surface markers, EpCAM (clone G8.8; Biolegend) and CD45 (clone 30-F11; Biolegend). Cells were
434 subsequently fixed with 2% paraformaldehyde/PBS (10min, RT), and blocked/permeablized in 0.2% Triton
435 X/PBS with 2% normal goat serum (20min, RT). Fixed and permeabilized cells were probed for
436 intracellular viral antigen with 2 distinct antibodies: Rabbit polyclonal anti-NS1/2 (a gift from Dr. Vernon
437 Ward, U. of Otago, Australia) and mouse monoclonal anti-NS1 (clone CM79, a gift from Dr. Ian Clark, U.
438 of Southampton, UK). These unconjugated antibodies were detected with anti-Rabbit Alexa Fluor 647
439 (Molecular Probes, Eugene, OR), and anti-mouse Dylight 405 (Jackson ImmunoResearch), respectively.
440 Cells were analyzed via flow cytometry, and viable cells that were EpCAM+, CD45-, NS1/2 pAb+, and
441 NS1 mAb+ were labeled as infected epithelial cells.
442
443 **RNA *in situ* hybridization via RNAscope®**
444 Sections of approximately two cm from the ileum that contained a Peyer's patch (PP) were selected,
445 cut open lengthwise, pinned apical side up in wax trays, and fixed in 10% neutral-buffered formalin (Sigma)
446 (18-24h, RT), then moved to 70% EtOH. Tissues were embedded in 2% agar (ThermoFisher), the PP was
447 vertically transected, flipped 90 degrees, and re-embedded in 2% agar. Agar blocks were maintained in
448 70% EtOH prior to being paraffin-embedded. Tissue sections (5um) were cut and maintained at RT with
449 desiccant until processed. RNA *in situ* hybridization was performed using the RNAscope Multiplex
450 Fluorescent v2 kit (Advanced Cell Diagnostics [ACDBio], Newark, CA) per protocol guidelines. Probes
451 were designed by ACDBio for detection of CW3 genomic RNA (471891-C1), CR6 genomic RNA (502631-
452 C1), and EpCAM mRNA (418151-C2), and signals were amplified and detected via ACDBio protocols
453 using TSA® plus technology (Perkin Elmer, Waltham, MA). Slides were mounted with ProLong Gold
454 antifade reagent (ThermoFisher), and imaged using a Zeiss ApoTome2 on an Axio Imager, with a Zeiss
455 AxioCam 506 (Zeiss, Jena, Germany).
456
457 **Statistical Analyses**

458 Data were analyzed with Prism 7 software (GraphPad Prism Software, La Jolla, CA), with specified
459 tests and significance noted in the figure legend.
460
461

Acknowledgements:

The authors would like to thank the OHSU Advanced Light Microscopy Core, Flow Cytometry Core, and Histopathology Shared Resource for technical support, Lena Li for overseeing mouse colonies, Stephanie Karst for guidance with RNAscope techniques, and Jacob VanWinkle for manuscript review and editing.

467 REFERENCES

468 1. Ahmed SM, Hall AJ, Robinson AE, Verhoef L, Premkumar P, Parashar UD, et al. Global
469 prevalence of norovirus in cases of gastroenteritis: a systematic review and meta-analysis. Lancet
470 Infect Dis. 2014;14: 725–730. doi:10.1016/S1473-3099(14)70767-4

471 2. Glass RI, Parashar UD, Estes MK. Norovirus gastroenteritis. N Engl J Med. 2009;361: 1776–1785.
472 doi:10.1056/NEJMra0804575

473 3. Saito M, Goel-Apaza S, Espetia S, Velasquez D, Cabrera L, Loli S, et al. Multiple norovirus
474 infections in a birth cohort in a Peruvian Periurban community. Clin Infect Dis. 2014;58: 483–491.
475 doi:10.1093/cid/cit763

476 4. Teunis PFM, Sukhrie FHA, Vennema H, Bogerman J, Beersma MFC, Koopmans MPG. Shedding
477 of norovirus in symptomatic and asymptomatic infections. Epidemiol Infect. 2015;143: 1710–1717.
478 doi:10.1017/S095026881400274X

479 5. Ettayebi K, Crawford SE, Murakami K, Broughman JR, Karandikar U, Tenge VR, et al.
480 Replication of human noroviruses in stem cell-derived human enteroids. Science. 2016.
481 doi:10.1126/science.aaf5211

482 6. Jones MK, Watanabe M, Zhu S, Graves CL, Keyes LR, Grau KR, et al. Enteric bacteria promote
483 human and mouse norovirus infection of B cells. Science. 2014;346: 755–759.
484 doi:10.1126/science.1257147

485 7. Karst SM, Wobus CE. A working model of how noroviruses infect the intestine. PLoS Pathog.
486 2015;11: e1004626. doi:10.1371/journal.ppat.1004626

487 8. Nice TJ, Robinson BA, Van Winkle JA. The Role of Interferon in Persistent Viral Infection:
488 Insights from Murine Norovirus. Trends Microbiol. 2017. doi:10.1016/j.tim.2017.10.010

489 9. Baldridge MT, Turula H, Wobus CE. Norovirus Regulation by Host and Microbe. Trends Mol
490 Med. 2016;22: 1047–1059. doi:10.1016/j.molmed.2016.10.003

491 10. Sosnovtsev SV, Belliot G, Chang K-O, Prikhodko VG, Thackray LB, Wobus CE, et al. Cleavage
492 map and proteolytic processing of the murine norovirus nonstructural polyprotein in infected cells.
493 J Virol. 2006;80: 7816–7831. doi:10.1128/JVI.00532-06

494 11. Karst SM, Wobus CE, Lay M, Davidson J, Virgin HW. STAT1-dependent innate immunity to a
495 Norwalk-like virus. Science. 2003;299: 1575–1578. doi:10.1126/science.1077905

496 12. Lambden PR, Caul EO, Ashley CR, Clarke IN. Sequence and genome organization of a human
497 small round-structured (Norwalk-like) virus. Science. 1993;259: 516–519.

498 13. McFadden N, Bailey D, Carrara G, Benson A, Chaudhry Y, Shortland A, et al. Norovirus
499 regulation of the innate immune response and apoptosis occurs via the product of the alternative
500 open reading frame 4. PLoS Pathog. 2011;7: e1002413. doi:10.1371/journal.ppat.1002413

501 14. Baker ES, Luckner SR, Krause KL, Lambden PR, Clarke IN, Ward VK. Inherent structural
502 disorder and dimerisation of murine norovirus NS1-2 protein. PLoS ONE. 2012;7: e30534.
503 doi:10.1371/journal.pone.0030534

504 15. Nice TJ, Strong DW, McCune BT, Pohl CS, Virgin HW. A single-amino-acid change in murine
505 norovirus NS1/2 is sufficient for colonic tropism and persistence. J Virol. 2013;87: 327–334.
506 doi:10.1128/JVI.01864-12

507 16. Bailey D, Thackray LB, Goodfellow IG. A single amino acid substitution in the murine norovirus
508 capsid protein is sufficient for attenuation in vivo. J Virol. 2008;82: 7725–7728.
509 doi:10.1128/JVI.00237-08

510 17. Strong DW, Thackray LB, Smith TJ, Virgin HW. Protruding domain of capsid protein is necessary
511 and sufficient to determine murine norovirus replication and pathogenesis in vivo. J Virol. 2012;86:
512 2950–2958. doi:10.1128/JVI.07038-11

513 18. Wilen CB, Lee S, Hsieh LL, Orchard RC, Desai C, Hykes BL, et al. Tropism for tuft cells
514 determines immune promotion of norovirus pathogenesis. Science. 2018;360: 204–208.
515 doi:10.1126/science.aar3799

516 19. Wobus CE, Karst SM, Thackray LB, Chang K-O, Sosnovtsev SV, Belliot G, et al. Replication of
517 Norovirus in cell culture reveals a tropism for dendritic cells and macrophages. PLoS Biol. 2004;2:
518 e432. doi:10.1371/journal.pbio.0020432

519 20. Grau KR, Roth AN, Zhu S, Hernandez A, Colliou N, DiVita BB, et al. The major targets of acute
520 norovirus infection are immune cells in the gut-associated lymphoid tissue. Nat Microbiol. 2017;2:
521 1586–1591. doi:10.1038/s41564-017-0057-7

522 21. Orchard RC, Wilen CB, Doench JG, Baldridge MT, McCune BT, Lee Y-CJ, et al. Discovery of a
523 proteinaceous cellular receptor for a norovirus. Science. 2016. doi:10.1126/science.aaf1220

524 22. Haga K, Fujimoto A, Takai-Todaka R, Miki M, Doan YH, Murakami K, et al. Functional receptor
525 molecules CD300lf and CD300ld within the CD300 family enable murine noroviruses to infect
526 cells. Proc Natl Acad Sci USA. 2016;113: E6248–E6255. doi:10.1073/pnas.1605575113

527 23. Hoffmann H-H, Schneider WM, Rice CM. Interferons and viruses: an evolutionary arms race of
528 molecular interactions. Trends Immunol. 2015;36: 124–138. doi:10.1016/j.it.2015.01.004

529 24. Nice TJ, Osborne LC, Tomov VT, Artis D, Wherry EJ, Virgin HW. Correction: Type I Interferon
530 Receptor Deficiency in Dendritic Cells Facilitates Systemic Murine Norovirus Persistence Despite
531 Enhanced Adaptive Immunity. PLoS Pathog. 2016;12: e1005684.
532 doi:10.1371/journal.ppat.1005684

533 25. Thackray LB, Duan E, Lazear HM, Kambal A, Schreiber RD, Diamond MS, et al. Critical role for
534 interferon regulatory factor 3 (IRF-3) and IRF-7 in type I interferon-mediated control of murine
535 norovirus replication. J Virol. 2012;86: 13515–13523. doi:10.1128/JVI.01824-12

536 26. Nice TJ, Baldridge MT, McCune BT, Norman JM, Lazear HM, Artyomov M, et al. Interferon-λ
537 cures persistent murine norovirus infection in the absence of adaptive immunity. Science.
538 2015;347: 269–273. doi:10.1126/science.1258100

539 27. Baldridge MT, Lee S, Brown JJ, McAllister N, Urbanek K, Dermody TS, et al. Expression of Ifnlr1
540 on Intestinal Epithelial Cells Is Critical to the Antiviral Effects of Interferon Lambda against
541 Norovirus and Reovirus. J Virol. 2017;91. doi:10.1128/JVI.02079-16

542 28. Lee S, Wilen CB, Orvedahl A, McCune BT, Kim K-W, Orchard RC, et al. Norovirus Cell Tropism
543 Is Determined by Combinatorial Action of a Viral Non-structural Protein and Host Cytokine. Cell
544 Host Microbe. 2017;22: 449–459.e4. doi:10.1016/j.chom.2017.08.021

545 29. Taylor RC, Cullen SP, Martin SJ. Apoptosis: controlled demolition at the cellular level. Nat Rev
546 Mol Cell Biol. 2008;9: 231–241. doi:10.1038/nrm2312

547 30. Galluzzi L, Brenner C, Morselli E, Touat Z, Kroemer G. Viral control of mitochondrial apoptosis.
548 PLoS Pathog. 2008;4: e1000018. doi:10.1371/journal.ppat.1000018

549 31. Polster BM, Pevsner J, Hardwick JM. Viral Bcl-2 homologs and their role in virus replication and
550 associated diseases. Biochim Biophys Acta. 2004;1644: 211–227.
551 doi:10.1016/j.bbamcr.2003.11.001

552 32. Tran AT, Cortens JP, Du Q, Wilkins JA, Coombs KM. Influenza virus induces apoptosis via BAD-
553 mediated mitochondrial dysregulation. J Virol. 2013;87: 1049–1060. doi:10.1128/JVI.02017-12

554 33. Tripathi S, Batra J, Cao W, Sharma K, Patel JR, Ranjan P, et al. Influenza A virus nucleoprotein
555 induces apoptosis in human airway epithelial cells: implications of a novel interaction between
556 nucleoprotein and host protein Clusterin. Cell Death Dis. 2013;4: e562. doi:10.1038/cddis.2013.89

557 34. Amara A, Mercer J. Viral apoptotic mimicry. Nat Rev Microbiol. 2015;13: 461–469.
558 doi:10.1038/nrmicro3469

559 35. Richard A, Tulasne D. Caspase cleavage of viral proteins, another way for viruses to make the best
560 of apoptosis. Cell Death Dis. 2012;3: e277. doi:10.1038/cddis.2012.18

561 36. Mebratu YA, Tipper J, Chand HS, Walton S, Harrod KS, Tesfaigzi Y. Bik Mediates Caspase-
562 Dependent Cleavage of Viral Proteins to Promote Influenza A Virus Infection. Am J Respir Cell
563 Mol Biol. 2016;54: 664–673. doi:10.1165/rcmb.2015-0133OC

564 37. Al-Molawi N, Beardmore VA, Carter MJ, Kass GEN, Roberts LO. Caspase-mediated cleavage of
565 the feline calicivirus capsid protein. J Gen Virol. 2003;84: 1237–1244. doi:10.1099/vir.0.18840-0

566 38. Cheetham S, Souza M, Meulia T, Grimes S, Han MG, Saif LJ. Pathogenesis of a genogroup II
567 human norovirus in gnotobiotic pigs. J Virol. 2006;80: 10372–10381. doi:10.1128/JVI.00809-06

568 39. Troeger H, Loddenkemper C, Schneider T, Schreier E, Epple H-J, Zeitz M, et al. Structural and
569 functional changes of the duodenum in human norovirus infection. Gut. 2009;58: 1070–1077.
570 doi:10.1136/gut.2008.160150

571 40. Mumphrey SM, Changotra H, Moore TN, Heimann-Nichols ER, Wobus CE, Reilly MJ, et al.
572 Murine norovirus 1 infection is associated with histopathological changes in immunocompetent
573 hosts, but clinical disease is prevented by STAT1-dependent interferon responses. J Virol. 2007;81:
574 3251–3263. doi:10.1128/JVI.02096-06

575 41. Bok K, Prikhodko VG, Green KY, Sosnovtsev SV. Apoptosis in murine norovirus-infected
576 RAW264.7 cells is associated with downregulation of survivin. J Virol. 2009;83: 3647–3656.
577 doi:10.1128/JVI.02028-08

578 42. Furman LM, Maaty WS, Petersen LK, Ettayebi K, Hardy ME, Bothner B. Cysteine protease

579 activation and apoptosis in Murine norovirus infection. Virol J. 2009;6: 139. doi:10.1186/1743-
580 422X-6-139

581 43. Herod MR, Salim O, Skilton RJ, Prince CA, Ward VK, Lambden PR, et al. Expression of the
582 murine norovirus (MNV) ORF1 polyprotein is sufficient to induce apoptosis in a virus-free cell
583 model. PLoS ONE. 2014;9: e90679. doi:10.1371/journal.pone.0090679

584 44. Chang HY, Yang X. Proteases for cell suicide: functions and regulation of caspases. Microbiol Mol
585 Biol Rev. 2000;64: 821–846.

586 45. Hyde JL, Sosnovtsev SV, Green KY, Wobus C, Virgin HW, Mackenzie JM. Mouse norovirus
587 replication is associated with virus-induced vesicle clusters originating from membranes derived
588 from the secretory pathway. J Virol. 2009;83: 9709–9719. doi:10.1128/JVI.00600-09

589 46. Hyde JL, Mackenzie JM. Subcellular localization of the MNV-1 ORF1 proteins and their potential
590 roles in the formation of the MNV-1 replication complex. Virology. 2010;406: 138–148.
591 doi:10.1016/j.virol.2010.06.047

592 47. Doerflinger SY, Cortese M, Romero-Brey I, Menne Z, Tubiana T, Schenk C, et al. Membrane
593 alterations induced by nonstructural proteins of human norovirus. PLoS Pathog. 2017;13:
594 e1006705. doi:10.1371/journal.ppat.1006705

595 48. McCune BT, Tang W, Lu J, Eaglesham JB, Thorne L, Mayer AE, et al. Noroviruses Co-opt the
596 Function of Host Proteins VAPA and VAPB for Replication via a Phenylalanine-Phenylalanine-
597 Acidic-Tract-Motif Mimic in Nonstructural Viral Protein NS1/2. MBio. 2017;8.
598 doi:10.1128/mBio.00668-17

599 49. Ettayebi K, Hardy ME. Norwalk virus nonstructural protein p48 forms a complex with the SNARE
600 regulator VAP-A and prevents cell surface expression of vesicular stomatitis virus G protein. J
601 Virol. 2003;77: 11790–11797.

602 50. Feng Z, Hensley L, McKnight KL, Hu F, Madden V, Ping L, et al. A pathogenic picornavirus
603 acquires an envelope by hijacking cellular membranes. Nature. 2013;496: 367–371.
604 doi:10.1038/nature12029

605 51. Chen Y-H, Du W, Hagemeijer MC, Takvorian PM, Pau C, Cali A, et al. Phosphatidylserine
606 vesicles enable efficient en bloc transmission of enteroviruses. Cell. 2015;160: 619–630.
607 doi:10.1016/j.cell.2015.01.032

608 52. Bhattacharyya S, Zagórska A, Lew ED, Shrestha B, Rothlin CV, Naughton J, et al. Enveloped
609 viruses disable innate immune responses in dendritic cells by direct activation of TAM receptors.
610 Cell Host Microbe. 2013;14: 136–147. doi:10.1016/j.chom.2013.07.005

611 53. Gerbe F, Legraverend C, Jay P. The intestinal epithelium tuft cells: specification and function. Cell
612 Mol Life Sci. 2012;69: 2907–2917. doi:10.1007/s00018-012-0984-7

613 54. Delgado ME, Grabinger T, Brunner T. Cell death at the intestinal epithelial front line. FEBS J.
614 2016;283: 2701–2719. doi:10.1111/febs.13575

615 55. Reginato MJ, Mills KR, Paulus JK, Lynch DK, Sgroi DC, Debnath J, et al. Integrins and EGFR
616 coordinately regulate the pro-apoptotic protein Bim to prevent anoikis. Nat Cell Biol. 2003;5: 733–

617 740. doi:10.1038/ncb1026

618 56. Hausmann M, Leucht K, Ploner C, Kiessling S, Villunger A, Becker H, et al. BCL-2 modifying
619 factor (BMF) is a central regulator of anoikis in human intestinal epithelial cells. J Biol Chem.
620 2011;286: 26533–26540. doi:10.1074/jbc.M111.265322

621 57. Youle RJ, Strasser A. The BCL-2 protein family: opposing activities that mediate cell death. Nat
622 Rev Mol Cell Biol. 2008;9: 47–59. doi:10.1038/nrm2308

623 58. Poon IKH, Lucas CD, Rossi AG, Ravichandran KS. Apoptotic cell clearance: basic biology and
624 therapeutic potential. Nat Rev Immunol. 2014;14: 166–180. doi:10.1038/nri3607

625 59. Lee CS, Penberthy KK, Wheeler KM, Juncadella IJ, Vandenabeele P, Lysiak JJ, et al. Boosting
626 Apoptotic Cell Clearance by Colonic Epithelial Cells Attenuates Inflammation In Vivo. Immunity.
627 2016;44: 807–820. doi:10.1016/j.immuni.2016.02.005

628 60. Juncadella IJ, Kadl A, Sharma AK, Shim YM, Hochreiter-Hufford A, Borish L, et al. Apoptotic
629 cell clearance by bronchial epithelial cells critically influences airway inflammation. Nature.
630 2013;493: 547–551. doi:10.1038/nature11714

631 61. Monks J, Rosner D, Geske FJ, Lehman L, Hanson L, Neville MC, et al. Epithelial cells as
632 phagocytes: apoptotic epithelial cells are engulfed by mammary alveolar epithelial cells and repress
633 inflammatory mediator release. Cell Death Differ. 2005;12: 107–114. doi:10.1038/sj.cdd.4401517

634 62. Blasi E, Barluzzi R, Bocchini V, Mazzolla R, Bistoni F. Immortalization of murine microglial cells
635 by a v-raf/v-myc carrying retrovirus. J Neuroimmunol. 1990;27: 229–237.

636 63. Qin Z, Noffz G, Mohaupt M, Blankenstein T. Interleukin-10 prevents dendritic cell accumulation
637 and vaccination with granulocyte-macrophage colony-stimulating factor gene-modified tumor
638 cells. J Immunol. 1997;159: 770–776.

639

640

641

642

643

644

645

646

647

648

649 **Figure Legends**

650 **Fig 1. MNV NS1/2 is cleaved by host caspases at late times-post-infection**. (A) Schematic of MNV
651 genomic organization, illustrating initial NS1/2 expression within the ORF1 polyprotein. Cleavage sites in
652 ORF1 are marked accordingly - sites cleaved by the viral protease (**v**) and sites cleaved by host caspases
653 (*), the latter at aspartic acid residues 121 and 131 within the 2 functional caspase motifs, $DKAD^{121}$ and
654 $DAMD^{131}$ [10]. (B) Schematic representation of the five MNV clones used in these studies. Clones with
655 $D_{121}G$ and $D_{131}G$ mutations are referred to as Δcasp, and indicated by the X. (C) BV2 cells were infected
656 with indicated strains of MNV (MOI=1), and whole cell extracts (WCE) were analyzed via western blot
657 (WB) at indicated times post-infection. Image is representative of 4 independent experiments. Arrows are
658 pointing to the full-length NS1/2 at ~45kD, and NS2 at ~28kD. * Denotes a non-specific band at ~30kD.
659 (D) BV2 cells were infected as in C, but subsequently treated with 50uM ZVAD-fmk at 10hpi, and WCE
660 were analyzed via WB. Image is representative of 3 independent experiments. SS, staurosporine.

661

662 **Fig 2. Cleavage of NS1/2 is not required for MNV replication *in vitro*.** (A, B) BV2 cells were infected
663 with the indicated strain of MNV (MOI=1) and infectious virus was analyzed at indicated times post-
664 infection via plaque assay. Data are an average of 3 independent experiments. WT (C, D) or *Stat1*$^{-/-}$ (E, F)
665 BMDCs were generated as described in methods, and infected and analyzed as in A-B. Data are an average
666 of 2 independent experiments. Dotted lines indicate limit of detection. Statistical significance was
667 determined via two-way ANOVA with Bonferroni's multiple comparisons test. *, $p \leq 0.05$. BMDCs, bone
668 marrow-derived dendritic cells.

669

670 **Fig 3. Cleavage of NS1/2 is specifically required for early replication in intestinal tissues.** WT B6
671 mice were perorally infected with indicated viruses (1e6 PFU). At 3 days post-infection (dpi), tissues (A,
672 B) and stool (C, D) were harvested and analyzed via plaque assay. Data are from 8-9 individual mice within
673 3 separate experiments, and mean values are indicated. (E-H) Peyer's patches within the ileum were

674 analyzed via RNA *in situ* hybridization, using RNAscope commercial protocols and probes. MNV genomic
675 RNA was probed within ORF2, which encodes the major capsid (VP1), and is labeled in magenta, epithelial
676 cells were probed via EpCAM, and labeled in green, and DAPI is labeling nuclei in blue. Images are
677 representative of 2-3 mice for each group. (I) Mice (5-6 per group) were infected with indicated virus and
678 survival was plotted over the course of 35 days. Statistical significance was determined via Mann-Whitney
679 test for A-D. *, $p \leq 0.05$; **, $p \leq 0.01$; ns, not significant; MLN, mesenteric lymph node; yellow scale
680 bar, 50μm; white scale bar, 20 μm.
681
682 **Fig 4. Cleavage of NS1/2 is critical for persistent infection in the intestine.** (A, B) WT B6 mice were
683 perorally infected with indicated viruses, sacrificed at 21 days post-infection (dpi), and indicated tissues
684 were analyzed via RT-qPCR for MNV genomic RNA. Data are combined from 2 separate experiments
685 with data points representing individual mice, and mean values are indicated. (C, D) Fecal pellets were
686 also collected at 21 dpi, and similarly analyzed. Statistical significance was determined via Mann-Whitney
687 test. *, $p \leq 0.05$; **, $p \leq 0.01$; ns, not significant; MLN, mesenteric lymph node.
688
689 **Fig 5. Caspase cleavage of NS1/2 is required independent of the IFN-λ response.** WT (A, C) or *Ifnlr*$^{-}$
690 $^{/-}$ (B, D) mice were infected by oral gavage with either 1e6 PFU or 1e7 PFU, as indicated. Fecal samples
691 (A, B) were collected at 3, 7, 14, and 21 days post-infection (dpi), and colon tissue (C, D) was harvested at
692 21dpi. All samples were analyzed via RT-qPCR, and the mean of each group (N=4) is indicated. Dotted
693 lines indicate limit of detection.
694
695 **Fig 6. NS1/2 cleavage is necessary for infection of intestinal epithelial cells.** (A-C) Littermate mice
696 deficient for the type III IFN receptor (*Ifnlr1*$^{-/-}$ or *Ifnlr1*$^{-/-}$/*Ifnar*$^{+/-}$, "LRKO"), deficient for both type I and
697 III IFN receptors (*Ifnlr1*$^{-/-}$/*Ifnar*$^{-/-}$, "DKO"), and matched receptor-sufficient controls (*Iflr1*$^{+/+}$ / *Ifnar*$^{+/+}$ or
698 *Iflr1*$^{+/-}$/*Ifnar*$^{+/-}$, "WT") were infected with indicated viruses (9-13 mice per group combined from 3 separate

699 experiments), and analyzed at 3 dpi. (A) Peyer's patches were collected and analyzed via RT-qPCR for
700 MNV genomic RNA and normalized to RPS29. (B, C) Intestinal epithelial cells (CD45-, EpCAM+) were
701 collected and doubly stained for NS1/2 as described in methods. Dotted line indicates limit of detection.
702 (C) Flow plots representing data from 5 mice in B (each mouse is a separate color). (D-F) Ileum tissue
703 from CR6-infected or $CR6_{\Delta casp}$-infected WT mice was analyzed via RNAscope at 3 dpi, as in Figure 3.
704 MNV RNA is in magenta, EpCAM is in green, and nuclei are stained with DAPI in blue. Images are
705 representative of 5 mice infected with each virus. white scale bar, 20μm. Legend refers to data in A and
706 B. Statistical significance was determined by Mann-Whitney test. *, $p \leq 0.05$.
707
708 **Fig 7. Cleavage of NS1/2 potentiates apoptotic cell death.** BV2 cells were infected (MOI=1) with
709 indicated MNV strains, and (A-D) whole cell extracts were collected at indicated times and analyzed via
710 WB for caspase 3, PARP, actin, and MNV ProPol. (A, D) Arrows denote cleaved fragments of caspase 3
711 and PARP, indicating activation. Images are representative of 3 independent experiments. Cleaved caspase
712 3 (B), and ProPol (normalized to actin) (C) were analyzed via densitometry, with average and SD shown.
713 (E-H) Cells were harvested at 14h and 17hpi, stained with Annexin V and zombie LIVE/DEAD viability
714 stain, and analyzed via flow cytometry. (E) Representative flow plots are shown from one of six
715 independent experiments. (F) Total Annexin V+ cells were averaged at 17hpi, and individual and mean
716 values are indicated, and (G) live, Annexin V+ (bottom right quadrant of flow plots in E), and (H) dead,
717 Annexin V+ (top right quadrant of flow plots in E) populations were also analyzed separately. Statistical
718 significance was determined by repeated measures one-way ANOVA, with Bonferroni's multiple
719 comparison test. *, $p \leq 0.05$; **, $p \leq 0.01$; ns, not significant. SS, staurosporine.

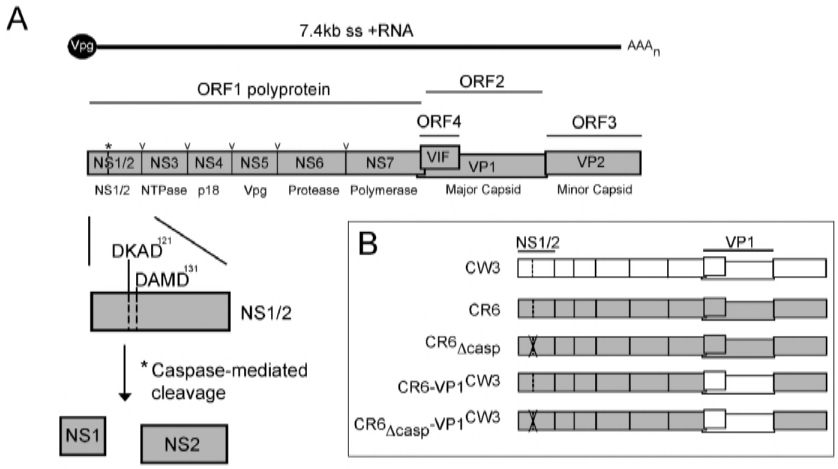
A
7.4kb ss +RNA
Vpg
AAA$_n$
ORF1 polyprotein
ORF2
ORF4
ORF3
NS1/2
NS3
NS4
NS5
NS6
NS7
VIF
VP1
VP2
NS1/2
NTPase
p18
Vpg
Protease
Polymerase
Major Capsid
Minor Capsid
DKAD^{121}
DAMD^{131}
NS1/2
* Caspase-mediated cleavage
NS1
NS2
B
NS1/2
VP1
CW3
CR6
CR6$_{\Delta casp}$
CR6-VP1^{CW3}
CR6$_{\Delta casp}$-VP1^{CW3}

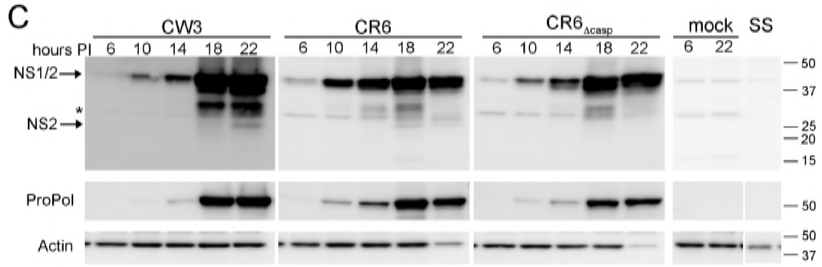
C
CW3
CR6
CR6$_{\Delta casp}$
mock
SS
hours PI
6 10 14 18 22
6 10 14 18 22
6 10 14 18 22
6 22
NS1/2
NS2
*
ProPol
Actin
50
37
25
20
15
50
50
37

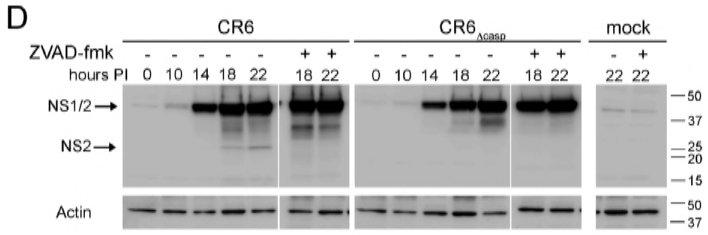
D
CR6
CR6$_{\Delta casp}$
mock
ZVAD-fmk
- - - - - + +
- - - - - + +
- +
hours PI
0 10 14 18 22 18 22
0 10 14 18 22 18 22
22 22
NS1/2
NS2
Actin
50
37
25
20
15
50
37

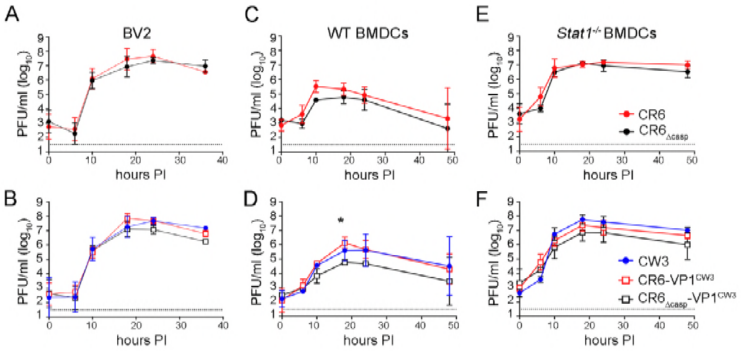
A
BV2
B
C
WT BMDCs
D
E
Stat1-/- BMDCs
F
PFU/ml (log10)
hours PI
CR6
CR6Δcasp
CW3
CR6-VP1CW3
CR6Δcasp-VP1CW3
*

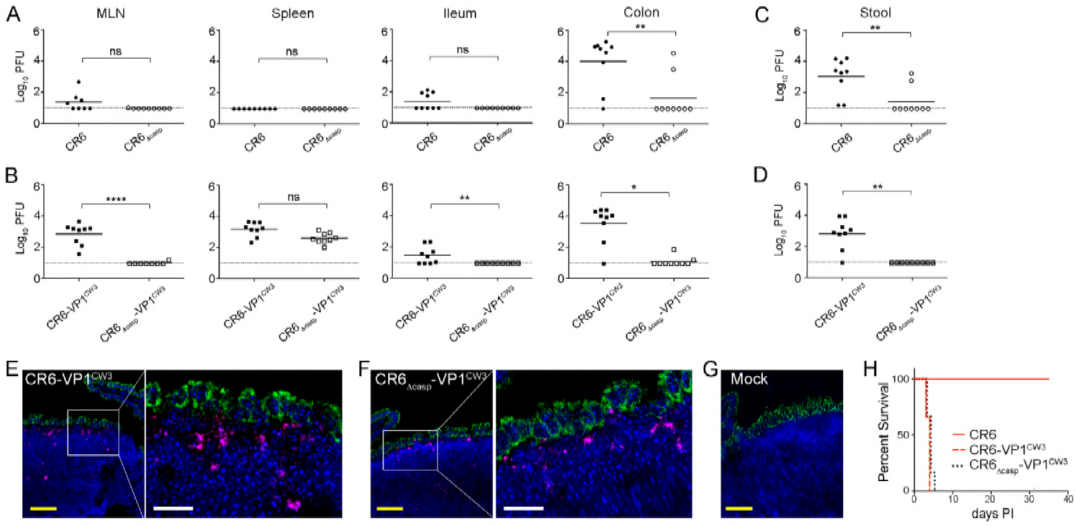
A
MLN
Spleen
Ileum
Colon
C
Stool
B
D
Log10 PFU
ns
**
****
*
CR6
CR6Δcasp
CR6-VP1CW3
CR6Δcasp-VP1CW3
E
F
G
H
Mock
Percent Survival
days PI
CR6
CR6-VP1CW3
CR6Δcasp-VP1CW3

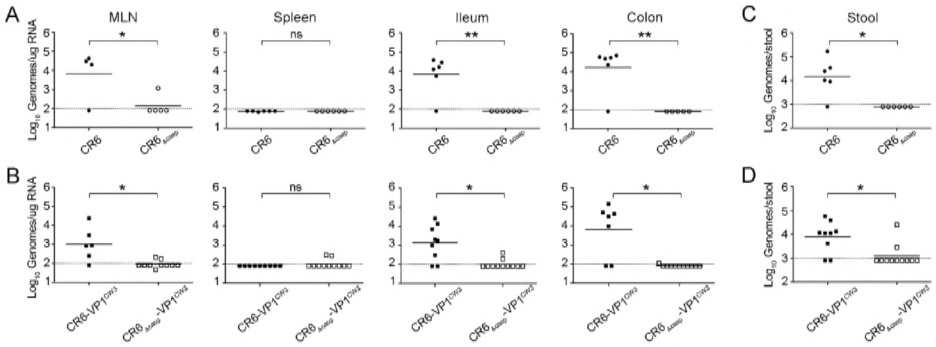
A
MLN
Spleen
Ileum
Colon
C
Stool
B
D
Log10 Genomes/ug RNA
Log10 Genomes/stool
CR6
CR6 Δcaep
CR6-VP1CW3
CR6 Δcaep-VP1CW3
*
ns
**

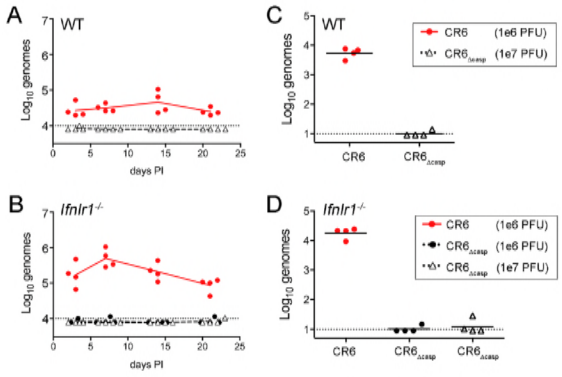
A
WT
Log10 genomes
days PI
B
Ifnlr1-/-
Log10 genomes
days PI
C
WT
Log10 genomes
CR6 (1e6 PFU)
CR6Δcasp (1e7 PFU)
CR6
CR6Δcasp
D
Ifnlr1-/-
Log10 genomes
CR6 (1e6 PFU)
CR6Δcasp (1e6 PFU)
CR6Δcasp (1e7 PFU)
CR6
CR6Δcasp
CR6Δcasp

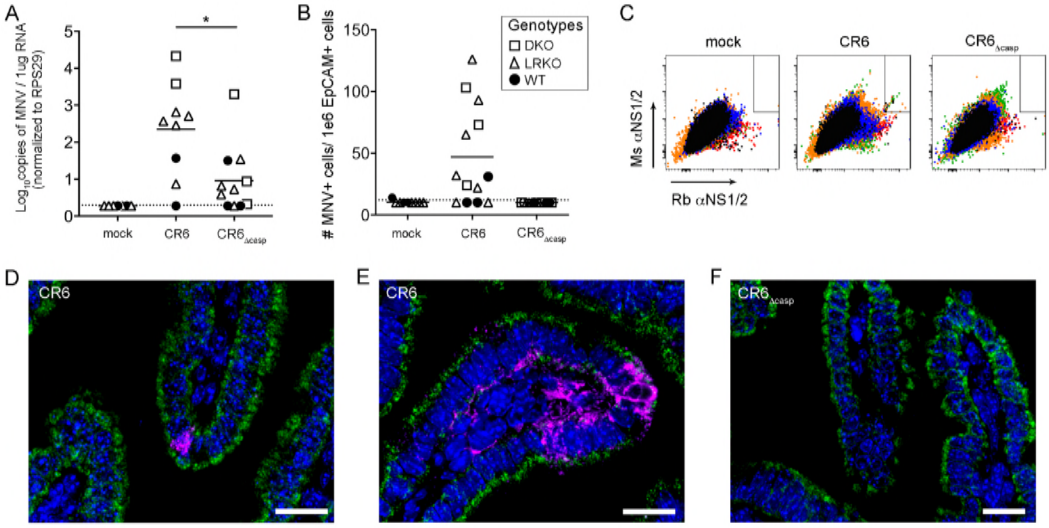
A
Log10 copies of MNV / 1ug RNA (normalized to RPS29)
*
mock
CR6
CR6Δcasp
B
MNV+ cells/ 1e6 EpCAM+ cells
Genotypes
DKO
LRKO
WT
mock
CR6
CR6Δcasp
C
mock
CR6
CR6Δcasp
Ms αNS1/2
Rb αNS1/2
D
CR6
E
CR6
F
CR6Δcasp

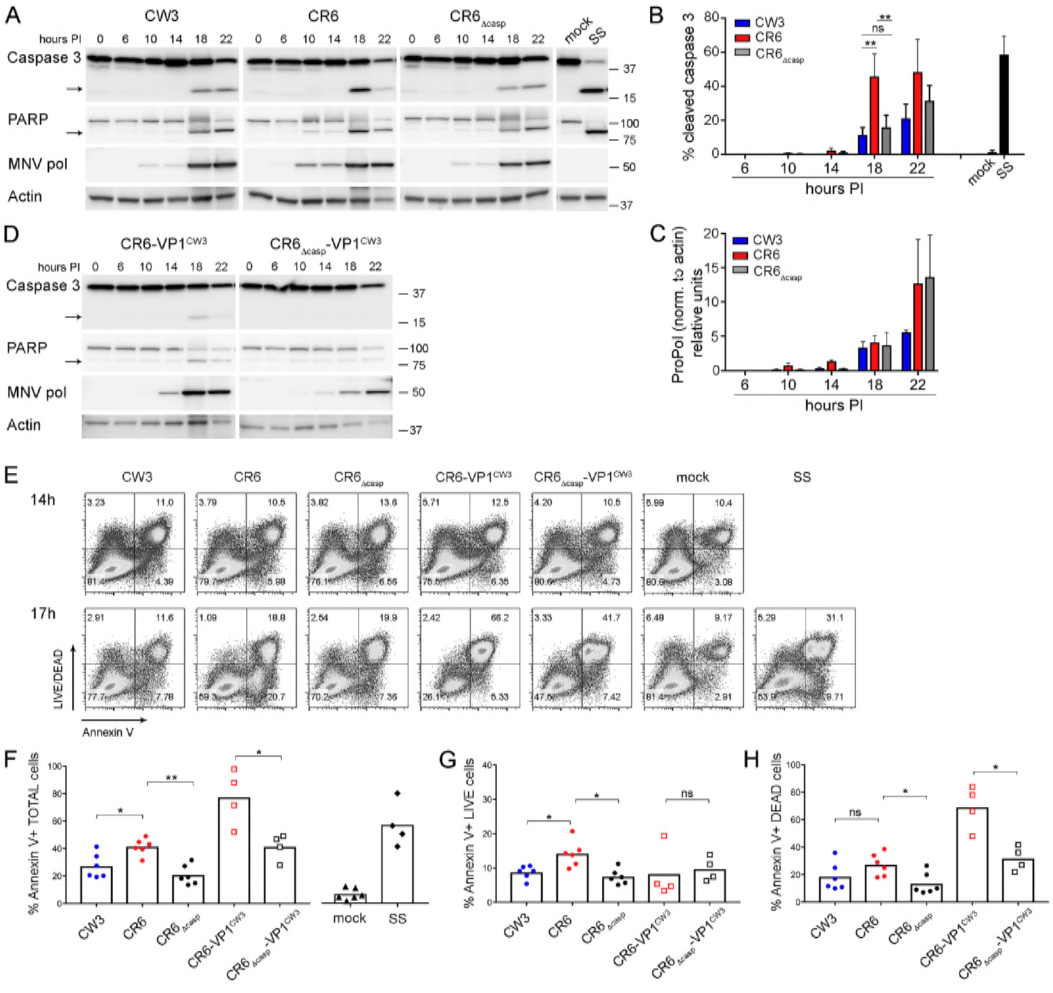
A
CW3
CR6
CR6Δcasp
hours PI
0 6 10 14 18 22
mock
SS
Caspase 3
PARP
MNV pol
Actin
37
15
100
75
50
37
B
CW3
CR6
CR6Δcasp
% cleaved caspase 3
ns
**
hours PI
mock
SS
C
ProPol (norm. to actin) relative units
hours PI
D
CR6-VP1CW3
CR6Δcasp-VP1CW3
E
CW3
CR6
CR6Δcasp
CR6-VP1CW3
CR6Δcasp-VP1CW3
mock
SS
14h
17h
LIVE/DEAD
Annexin V
F
% Annexin V+ TOTAL cells
G
% Annexin V+ LIVE cells
H
% Annexin V+ DEAD cells
ns